JACS
JOURNAL OF THE AMERICAN CHEMICAL SOCIETY

ARTICLE

pubs.acs.org/JACS

Electrocatalytic Monitoring of Metal Binding and Mutation-Induced Conformational Changes in p53 at Picomole Level

Emil Paleček,*[,†] Veronika Ostatná,[†] Hana Černocká,[†] Andreas C. Joerger,[‡] and Alan R. Fersht[‡]

[†]Institute of Biophysics, Academy of Sciences of the Czech Republic, v.v.i., Královopolská 135, 612 65 Brno, Czech Republic
[‡]MRC Laboratory of Molecular Biology, Cambridge CB2 0QH, U.K.

Supporting Information

ABSTRACT: We developed an innovative electrochemical method for monitoring conformational transitions in proteins using constant current chronopotentiometric stripping (CPS) with dithiothreitol-modified mercury electrodes. The method was applied to study the effect of oncogenic mutations on the DNA-binding domain of the tumor suppressor p53. The CPS responses of wild-type and mutant p53 showed excellent correlation with structural and stability data and provided additional insights into the differential dynamic behavior of the proteins. Further, we were able to monitor the loss of an essential zinc ion resulting from mutation (R175H) or metal chelation. We envisage that our CPS method can be applied to the analysis of virtually any protein as a sensor for conformational transitions or ligand binding to complement conventional techniques, but with the added benefit that only relatively small amounts of protein are needed and instant results are obtained. This work may lay the foundation for the wide application of electrochemistry in protein science, including proteomics and biomedicine.

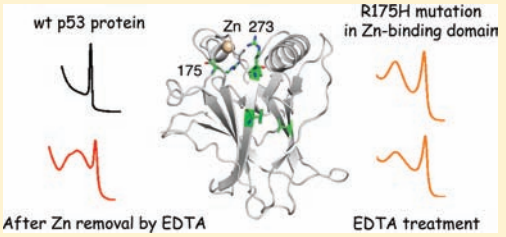

INTRODUCTION

The tumor suppressor protein p53 plays a critical role in the cellular response to DNA damage by regulating the expression of genes involved in controlling the cell cycle, DNA repair, and apoptosis.[1,2] It is directly inactivated by mutation in about 50% of human cancers, with most oncogenic mutations being located in the DNA-binding core domain of the protein.[3,4] It is essential to understand the molecular basis of p53 inactivation in cancer in order to develop novel anticancer strategies.[5] The structural effects of many oncogenic p53 mutants have been intensively studied by X-ray crystallography and complementary techniques (reviewed in ref 6). Yet, the most frequent cancer-associated mutant, R175H, which is highly destabilized, has eluded a detailed structural characterization so far, highlighting the need for complementary techniques to study conformationally unstable mutants.

In recent decades, electrochemistry of proteins was limited to relatively small conjugated proteins containing nonprotein redox centers yielding reversible electrochemistry,[7−10] and a majority of proteins were neglected. We have proposed a new electrochemical method for analysis of practically all proteins, which is sensitive to changes in protein structure.[11−20] This method is based on the ability of proteins to catalyze hydrogen evolution at mercury electrodes[19,21−23] and relies on constant current chronopotentiometric stripping (CPS; involving very fast potential changes) and mercury-containing electrodes.[15,24] With this method, a number of proteins in their native and denatured and/or reduced and oxidized forms were analyzed displaying protein structure-sensitive responses (denominated as peaks H).[11,15] We used CPS to study aggregation of α-synuclein (important in Parkinson's disease), and we detected changes in the interfacial behavior of this protein preceding fibril formation.[15]

To our knowledge, the only paper using electrochemical analysis to study the p53 protein was limited to determination of traces of glutathione-*S*-transferase in the C-terminal domain of p53.[25] Studies of the full-length p53 protein or its core domain were difficult because of DTT (dithiothreitol; usually present in these p53 samples), which interfered with the electroanalysis at mercury electrodes.[19] Replacement of DTT by other reducing agents, such as tris(2-carboxyl-ethyl)phosphine hydrochloride, was laborious, risking damaging the labile proteins. Recently, we have proposed thiol-modified mercury electrodes.[19] Thiol self-assembled monolayers (SAM) at the Hg surface do not interfere with the electrocatalytic reaction responsible for peak H and make analysis of reduced proteins (usually stored with mM concentrations of DTT) easier.

Here, we applied CPS in combination with DTT-modified HMDE (DTT-HMDE) to study the DNA-binding domain of human p53 and cancer-associated mutants. We observed striking differences between the CPS responses of the wild-type like protein T-p53C and its R175H mutant, which has a perturbed zinc-binding region. Removal of the zinc ion from T-p53C resulted in a CPS response resembling that of the R175H mutant. Studies of other T-p53C mutants showed some

Received: February 9, 2011
Published: April 14, 2011

dx.doi.org/10.1021/ja201006s | *J. Am. Chem. Soc.* 2011, 133, 7190–7196

correlation between the structure and stability of mutants and the CPS responses.

EXPERIMENTAL SECTION

Proteins and Materials. The low thermodynamic and kinetic stability of the wild-type p53 protein makes the protein difficult to study by biophysical and structural methods. We therefore used a superstable variant of the p53 core domain, T-p53C, for all our measurements. T-p53C contains four stabilizing mutations in the core domain (M133L/V203A/N239Y/N268D), providing a more stable structural framework while retaining the overall structural and functional characteristics of the wild-type protein.[26,27] Various previously described T-p53C mutants were generated.[26,28−30] Briefly, mutations were introduced into the gene of the p53 DNA-binding domain using the QuikChange site-directed mutagenesis kit (Stratagene). The genes of T-p53C, T-p53-V143A, T-p53C-R175H, T-p53C-F270L, T-p53C-R273H were then overexpressed in *Escherichia coli*, and the mutant proteins were purified by cation exchange chromatography on a Sepharose SP column (GE Healthcare), affinity chromatography on HiTrap Heparin (GE Healthcare) and gel filtration on a Superdex 75 column (GE Healthcare) as the final purification step. Purified proteins were flash frozen and stored at −80 °C. All chemicals were of analytical grade, and solutions were prepared from triply distilled water.

Apparatus. Electrochemical measurements were performed with an AUTOLAB Analyzer (EcoChemie, Utrecht, The Netherlands) in combination with VA-Stand 663 (Metrohm, Herisau, Switzerland); a 0.4 mm^2 hanging mercury drop electrode (HMDE) served as the working electrode in a standard cell in a three-electrode system. An Ag|AgCl|3 M KCl electrode was used as the reference electrode and a platinum wire as the auxiliary electrode. Experiments were carried out at controlled temperature (Julabo F 25-EH, ILABO, Czech republic), open to air.

Procedures. All experiments were performed using Adsorptive Transfer Stripping (AdTS, ex situ) technique.[15,31] The term "stripping" does not mean that the protein is literally stripped off the mercury electrode during the current application. It is used in the same connotation as, for example, in the case of the DNA adsorptive stripping,[32] in which DNA is first accumulated at the electrode surface followed by reduction of the accessible base residues. Strongly adsorbed nucleic acid molecules remain, however, at the electrode surface, even at potentials more negative than the reduction potential of adenine or cytosine residues.[33−35] Our preliminary results suggest that proteins, including the p53 core domain, also remain adsorbed at the surface at potentials slightly more negative than peak H. But, similarly to DNA,[31,34] some protein unfolding is taking place. This process depends on various factors, including the current density, end potential, and so forth. More details will be published elsewhere.

p53 proteins were adsorbed from 5 μL drops of p53 solution (20 mM Na-phosphate buffer, pH 7, 200 mM NaCl, and 5 mM DTT) at HMDE. The protein-modified electrode was washed and transferred to the blank background electrolyte in a thermostatted electrolytic cell, followed by recording of the chronopotentiogram. Measurements of p53 proteins were performed at a protein concentration of 2 μM and an accumulation time (t_A) of 60 s, that is, under surface saturation conditions where the CPS signals of the proteins depended little on protein concentrations or on t_A (Figure SI-4).

Theory. In this study, we used the catalytic hydrogen evolution reaction (CHER), which is the most sensitive electrochemical reaction for the analysis of proteins. The CHER can be satisfactorily described by the following equations:[36]

$$2PH_{(surf)} + 2e^- \leftrightarrows 2P^-_{(surf)} + H_{2(g)} \quad (1)$$

$$P^-_{(surf)} + BH_{(aq)} \leftrightarrows PH_{(surf)} + B^-_{(aq)} \quad (2)$$

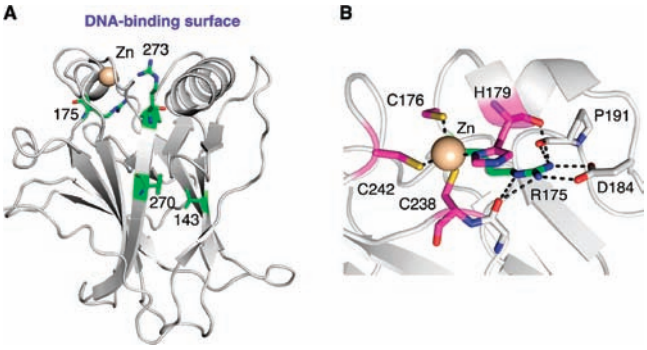

Figure 1. Structure of the DNA-binding domain of p53. (A) Overall structure of T-p53C (PDB entry 1UOL).[26] Sites of cancer mutations investigated in this study (V143A, R175H, F270L, and R273H) are highlighted as green stick models. The destabilizing V143A and F270L mutations create internal cavities in the hydrophobic core of the β-sandwich.[28] The contact mutation R273H removes an essential DNA-contact residue, with minimal effects on the overall structure and stability of the protein.[29] Arg175 is located next to the zinc-binding site, and mutation to a histidine is thought to perturb the zinc coordination sphere,[6] resulting in loss of the zinc ion. (B) Close-up view of the zinc coordination sphere, with the four zinc ligands shown in magenta. The polar interaction network mediated via the side chain of Arg175 (shown as green stick model) is highlighted by dashed lines. The figure was generated using PyMOL (www.pymol.org).

where PH and P^- represent protonated and unprotonated amino acid residues in the protein, respectively, while BH is the acid component of the buffer solution and B^- its conjugate base. The symbols in parentheses represent the state of the molecules (g stands for gaseous, aq for aqueous, and surf for surface confined). These reactions imply that the catalyst is the protein anchored to the surface of the electrode. This is the case particularly in our *ex situ* experiments (Figures 2−6) in which the protein-modified electrode is immersed in the blank background electrolyte (containing no protein in solution).

Additional Methods and Proteins. CPS peaks H of native and denatured BSA, parameters of peaks H of wt and mutant p53 proteins at different temperatures, and dependence of peak H on p53 concentration as well as voltammetric responses of wild-type and mutant p53 proteins at mercury and carbon electrodes are available in Supporting Information.

Abbreviations Used. AdS, adsorptive stripping (*in situ*); AdTS, adsorptive transfer stripping (*ex situ*); BSA, bovine serum albumin; CHER, catalytic hydrogen evolution reaction; CPS, constant current chronopotentiometric stripping; CV, cyclic voltammetry; DTT, dithiothreitol; DTT-HMDE, DTT-modified hanging mercury drop electrode; E_p, peak potential; EDTA, ethylenediaminetetraacetic acid; I_{str}, stripping current; peak H, CPS signal of proteins resulting from CHER; SAM, self-assembled monolayer; t_A, accumulation time; T-p53C, superstable variant of the p53 core domain; $W_{1/2}$, peak half-width; wt, wild-type.

RESULTS

CPS of Wild-Type T-p53C and Its R175H Mutant at Different Temperatures. We investigated electrochemical responses of wild-type (wt) T-p53C and its R175H mutant at temperatures between 8.6 and 20.3 °C. R175H is the most frequent p53 cancer mutation and is located in the L2 loop of the DNA-binding domain in direct vicinity of the zinc coordination sphere (Figure 1). The mutation is thought to induce substantial structural perturbation in the zinc-binding region, causing loss of the zinc ion and increased conformational flexibility.[6,37] As a result of mutation, the protein is destabilized by 3.5 kcal/mol and

loses its sequence-specific DNA-binding activity. Similar effects are observed for the wild-type protein upon removal of the zinc ion with the chelating agent EDTA.[38]

Polarographic and voltammetric signals of low MW compounds, caused by hydrogen evolution catalyzed by surface-attached species, are often almost unaffected by changes in temperature[23] because in the usual (*in situ*) experiments an increase in the protonation rate constant with increasing temperature could be compensated by decreased adsorption of the catalyst at the electrode surface. In our experimental arrangement (*ex situ*), in which the protein is adsorbed from a drop of solution at constant temperature (and the protein-modified electrode is transferred to the blank background electrolyte) and measured at different temperatures in an electrolytic cell, no effect of temperature-induced changes during adsorption can be expected. On the other hand, in the surface-attached protein molecules, changes in temperature (in the electrolytic cell) may reflect not only the rate of protonation, but also changes in the protein structure and dynamics, which in turn may affect accessibility of the amino acid residues involved in the electrode process. Figure 2 shows CPS curves of wt and mutant R175H measured between 8.6 and 20.3 °C. At 8.6 °C, wt T-p53C produced no peak, whereas the R175H mutant yielded a well-developed peak $H1^{175}$ at −1.90 V (Table SI−I). The height of peak $H1^{175}$ increased between 8.6 and 17.9 °C about 3.3-fold (Figure 2). An even larger increase was observed in peak $H1^{wt}$ of wt T-p53C after its appearance at temperatures above 11.1 °C (Figure 2C−F, Table SI−I). In contrast to p53, peaks of native and denatured BSA increased only by about 25% (Figure SI-1). The large increase in p53 peak heights (as compared to BSA) suggested that the electrocatalysis of the p53 proteins is governed by a lower conformational stability and/or faster dynamics. The peak potential (E_p) of both BSA and p53 shifted with increasing temperature to less negative values (Figure 2, Table SI−I, Figure SI-1), suggesting that at higher temperatures CHER is easier, requiring less energy for the electrode process. At 15.9 °C, a highly negative peak $H2^{175}$ appeared (Figure 2D, Table SI−I). At 17.9 °C, peak $H2^{175}$ became well developed and its E_p was only slightly more negative than that of peak $H1^{wt}$ (Figure 2E). At 20.3 °C, the E_p of $H2^{175}$ was almost the same as the E_p of $H1^{wt}$ at −1.91 V, but peak $H2^{175}$ was much broader (Figure.2F). The half-width ($W_{1/2}$) of this peak increased with temperature, in contrast to the decreasing $W_{1/2}$ of peak H1 (Figure 2, Table SI−I).

Clearly, CPS peak heights of both proteins strongly increased with temperature but differed greatly between wt T-p53C and the R175H mutant (Figure 2). The differences in CPS peaks of T-p53C and R175H resembled differences between peaks of native and denatured BSA (Figure SI-1). Different CPS responses observed in native and denatured proteins, as well as in reduced and oxidized peptides and proteins, were explained by differences in the accessibility of the proteins' catalytically active groups[12,15] and different organization of the protein or peptide layers at the electrode surface.[11,36] Structural differences between T-p53C proteins may influence the orientation of their molecules at the surface, which in turn can affect the accessibility of the catalytically active groups for the electrode processes. Considering the CPS behavior of native and denatured BSA[12−14,16,17,19] (Figure SI-1), the observed CPS responses of T-p53C and the highly destabilized R175H mutant (Figure 2) are thus not surprising.

It has been shown that arginine, lysine, and cysteine are catalytically active residues in proteins, polyamino acids, and

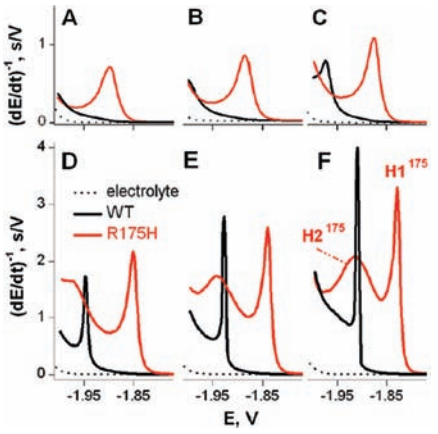

Figure 2. CPS peak H of wt T-p53C (black) and mutant R175H (red) at 8.6 °C (A), 11.1 °C (B), 13.9 °C (C), 15.9 °C (D), 17.9 °C (E), and 20.3 °C (F). p53 protein was adsorbed from a 5 μL drop of a 2 μM p53 solution (containing 5 mM DTT) at open circuit potential for t_A = 60 s at HMDE. Then, the p53-modified DTT-HMDE was washed and transferred into the electrolytic cell containing blank 50 mM sodium phosphate, pH 7.3, to perform CPS analysis at different temperatures; I_{str} =−30 μA.

peptides close to neutral pH.[15,36,39] Histidine residues behaved as very weak catalysts under these conditions. Each of these three residues alone in the polypeptide chain was sufficient to catalyze hydrogen evolution and produce peak H at mercury electrodes.[36,39] At low temperatures, electrocatalysis in native T-p53C may be inhibited because of reduced conformational flexibility of the protein (Figure 2A,B), preventing communication of catalytically active groups with the electrode. Absence of peak H in T-p53C (Figure 2A,B) at low temperature should not be explained by total electroinactivity of this protein. At lower current density, a relatively small peak H was observed (not shown), suggesting involvement of a fraction of accessible amino acid residues in the electrocatalysis, resulting probably from a small structural distortion at the site of the protein molecule adhering to the electrode surface. Much smaller CPS responses of wt T-p53C, compared to the well-developed peak H1 in R175H (Figure 2A−C), suggest that the mutant is a better catalyst, offering probably a greater number of amino acid residues for the electrocatalytic process. The structural perturbation of the mutant zinc-binding site, which contains three cysteines (see Figure 1B), is probably the main reason for the appearance of peak H1 in R175H at low temperatures (Figure 2A,B). Substitution of the catalytically active Arg175 in R175H by a less active His was not sufficient to compensate for the effects of the structural perturbation in the mutant. The broad peak $H2^{175}$ observed in R175H at 17.9 and 20.3 °C (Figure 2E,F) appeared neither in wt T-p53C (Figure 2) nor in BSA under the same conditions (Figure SI-1), but it appeared in wt T-p53C at higher temperatures (data not shown). More stable (native) BSA did not produce peak H2 even at 36 °C (Figure SI-1D) but denatured BSA yielded a broad H2 at −1.89 V and 26.4 °C (Figure SI-1C). Appearance of peak H2 in native proteins at higher temperatures might be due to structural reorganization of the protein molecules at the electrode surface, and thus reflects protein dynamics.

Other Methods. Cyclic voltammetry of wt T-p53C and R175H yielded catalytic peaks close to −1.9 V at scan rates between 10 mV and 2 V/s (Figure SI-2). Peaks of wt T-p53C and

R175H differed only little, in agreement with our earlier finding that at these scan rates the reduced DTT layer is disturbed and prolonged contact with the negatively charged bare mercury surface may result in denaturation of the protein.[13,14,19] On the other hand, in CPS at high current densities (inducing much faster potential changes than in the CV, Figure SI-2), even the reduced DTT layer remains sufficiently ordered at highly negative potentials to prevent protein contact with the bare electrode.[19] Square wave voltammetry of wt T-p53C and R175H with (bare) pyrolytic graphite electrode yielded at 15 °C oxidation peaks close to +0.8 V with only small difference in their heights (Figure SI-3). More work with different carbon electrodes will be necessary to find out whether these electrodes can be useful for studying p53 protein structures.

CPS Response of Structurally Similar p53 Mutants. We investigated the temperature-sensitive V143A and F270L cancer mutants, which are structurally and thermodynamically very similar. Both mutations create an internal cavity in the same region of hydrophobic core of the β-sandwich without collapse of the surrounding structure (see Figure 1). As a result, they have the same overall structure as the wild-type protein (i.e., T-p53C) but a much reduced thermodynamic stability.[28] Figure 3 shows CPS peaks of both mutants at temperatures between 15.9 and 22.7 °C. In this temperature range, the CPS responses of the two mutants were almost identical. At 15.9 and 17.9 °C, peak H1 of F270L was slightly higher than that of V143A (Figure 3A,B), which could be explained by a small stability difference between the two mutants,[28] although the observed differences are too small to draw final conclusions. The first sign of peak H2 appeared at 20.3 °C, that is, at a temperature where wt T-p53C did not display this peak. It increased at higher temperatures (Figure 3C−E), suggesting that CPS reflects the conformational stability of T-p53C proteins. Between 15.9 and 20.3 °C, peaks of F270L were slightly more negative than those of V143A (Figure 3A−C), although the difference was within the experimental error. Peaks $H2^{V143A}$ and $H2^{F270L}$ obtained at 22.7 °C (Figure 3E) were much narrower ($W_{1/2}$ 15 mV) than peak $H2^{R175H}$ of the R175H mutant (Figure 2E,F). Given that the molecular surfaces of V143A, F270L, and wild-type T-p53C are essentially identical in their crystal structure,[28] the different CPS response of the wild-type protein can be directly attributed to its increased thermostability and hence reduced conformational flexibility compared to the mutant proteins. Almost identical CPS responses (Figure 3) of the structurally and stability-wise very similar V143A and F270L mutants and the correlation of the CPS response with protein stability suggest a significant role of the p53C structure in the electrode processes.

Removal of Zinc from Wild-Type and Mutant Proteins. Zinc coordination is necessary for proper folding of the p53 core domain *in vitro* and *in vivo*.[40] We were interested in how the removal of the zinc ion from T-p53C and its mutants influences the CPS responses of the proteins and particularly whether the removal of zinc from the wt protein results in appearance of the broad peak H2 observed in R175H. Treatment of wt T-p53C with 0.5 or 5 mM EDTA for 10 min on ice resulted only in shifts of peak $H1^{wt}$ to positive potentials (ΔE_p 10 mV), while 20 mM EDTA produced a broad peak $H2^{wt}$ ($W_{1/2}$ 32 mV) at −1.94 V (Figure 4A). In contrast, the same EDTA treatment of R175H was almost without effect on its CPS peaks (Figure 4B), indicating that no zinc was bound in the R175H samples (or at least that

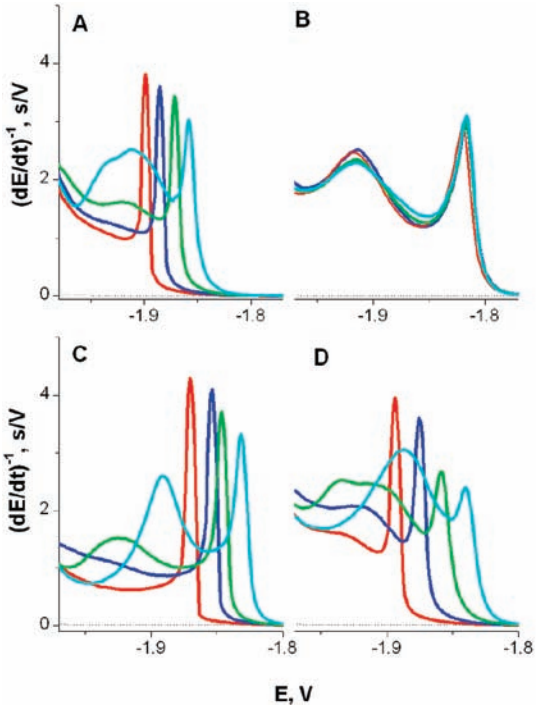

Figure 4. CPS peaks H of wt (A), R175H (B), R273H (C), and V143A (D) treated with 0 mM (red), 5 mM (blue), 10 mM (green), and 20 mM (cyan) EDTA at 0 °C for 10 min. CPS measurements were performed at 18 °C. More details are in the text and in Figure 2.

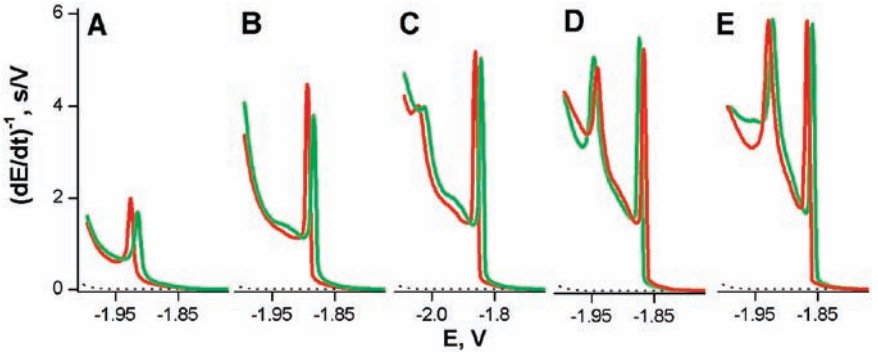

Figure 3. CPS peak H of p53 mutants F270L (red) and V143A (green) at 15.9 °C (A), 17.9 °C (B), 20.3 °C (C), 21.6 °C (D), and 22.7 °C (E). More details are in the text and in Figure 2.

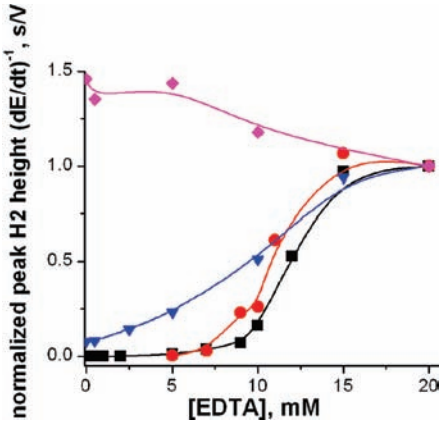

Figure 5. Dependence of normalized peak H2 height of wt (black), R273H (red), V143A (blue), and R175H (magenta) on the concentration of EDTA pretreatment at 26 °C. Peak H2 heights of wt and mutant T-p53C treated with 20 mM EDTA were taken as 1. Measurements were performed at 18 °C. More details are in the text and in Figure 4.

the population of zinc-bound molecules was negligible). The responses to the EDTA treatment of V143A and the DNA-contact mutant R273H (see Figure 1) were similar but not identical to those of T-p53C, showing some differences in the effect of 5 mM EDTA on their CPS peaks (Figure 4).

To obtain more detailed information about the CPS responses of these mutants upon EDTA treatment, we studied the effect of EDTA concentrations in greater detail as well as the effect of temperature on the measured CPS peaks. Treatment of the p53C proteins with different EDTA concentrations resulted in an E_p shift of peak H1 in wt and mutant proteins to less negative values (Figure 4), probably indicating gradual changes in the protein layers resulting from zinc interactions with EDTA and/or removal of zinc ions in some protein molecules. The heights of peak H2 of wt and mutant proteins depended on the EDTA concentration differently (Figures 4 and 5). The shapes of these dependencies of wt and R273H (Figure 5) resembled structural transition curves, with the midpoint of R273H shifted to lower EDTA concentrations as compared to the wt. In contrast, peak H2 of V143A (and F270L, not shown) increased almost linearly with the EDTA concentration, whereas no increase of H2 was observed in R175H. The small decrease of this peak at higher EDTA concentrations might be due to the tendency of this mutant to aggregate.

Figure 6 shows CPS peaks of untreated and 5 mM EDTA-treated wt and mutant proteins measured at different temperatures. As expected, the R175H mutant gave almost identical curves for EDTA-treated and untreated samples at a given temperature, whereas curves of EDTA-treated and untreated wt and two other mutants differed. The peak H1 heights of untreated wt and mutants increased with temperature, and the E_p values of the mutants were always less negative than the E_p of wt p53 (Figures 3 and 6). The largest difference between the E_p of wt and mutant peak H1 (90 mV at 13.5 °C) was observed for R175H, suggesting strong structural disturbance in this protein. R273H, structurally similar to the wt apart from the mutation (of an electrochemically active residue) on the protein surface, produced a peak H1 similar but not identical to the wt protein. Considering the peak height and E_p as well as the absence of peak H2, the CPS responses of this mutant were more similar to those of wt than to any other tested mutant. It is interesting to note that

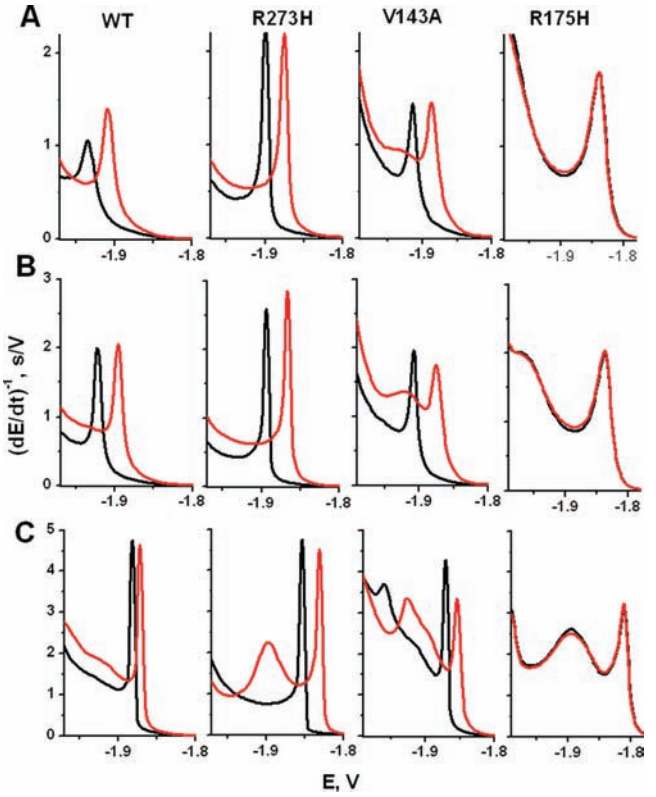

Figure 6. CPS peak H of 2 μM wt and mutants R273H, V143A, and R175H without (black) and with treatment with 5 mM EDTA (red) for 10 min at 0 °C. CPS analysis was performed at 13.9 °C (A), 15.3 °C (B), and 19.8 °C (C). More details are in the text and in Figure 2.

the mutations that affect the structural plasticity of the protein, while retaining the overall structure (V143A and F270L), had a much more pronounced effect on the CPS response than a structurally inert surface mutation (R273H), even with the latter affecting a residue that is theoretically electrocatalytically active.

Overall, comparison of the CPS responses with and without EDTA clearly shows that the R175H mutation impairs zinc binding of p53. EDTA treatment of the wt and R273H proteins had little effect on their CPS responses at low EDTA concentrations, but 10 mM EDTA induced the appearance of peak H2, suggesting the beginning of the structural transition upon zinc loss (Figure 5). Compared to the wt and R273H, in V143A much lower EDTA concentrations were needed to induce peak $H2^{V143A}$, indicating a greater conformational flexibility in the zinc region, even though the mutation site is distant from the zinc coordination sphere. As such, the CPS signal seems to respond to mutation-induced long-range effects on protein dynamics.

At this stage, we cannot explain p53 peaks and particularly peak H2 unequivocally. We can only tentatively suggest that the sharp peak H1 could be related to accessible electrocatalytically active groups in an ordered p53C layer. The broad peak H2 could involve distorted or partially unfolded regions, strongly influencing the protein layer structure at the electrode surface. The electrode process responsible for this peak requires higher temperatures (Figures 2 and 6) than for peak H1, observed already at 8.6 °C in R175H and 13.9 °C in wt T-p53C. Interestingly, this stability difference is in the same range as the difference in the melting temperatures of both proteins.[30]

Considering the relation between the appearance of peak H2 and the effect of the zinc removal from p53C by EDTA (Figures 4−6), we speculate that in R175H the cysteines in the perturbed zinc-binding site (Cys176, Cys238, and Cys242) significantly change the structure of the adsorbed protein layer and contribute to CHER.

DISCUSSION

To our knowledge, this is the first paper dealing with interfacial properties of wt and mutant p53 proteins. To obtain information about these properties of the p53 core domain, we combined: (a) CHER known as highly sensitive to the catalyst structure;[21−23] (b) CPS using high current densities (∼−7.5 mA/cm^2, at I_{str} −30 μA) and allowing very fast potential changes (∼250 V/s), critical for preventing protein denaturation at negatively charged surfaces; (c) DTT-modified mercury electrodes and (d) superstable variants of wt and mutant p53 core domain, for which high resolution structures are available, and which are better suited for physical chemical studies than the native p53 proteins. Our results showed large differences in the interfacial behavior of T-p53C and the R175H mutant (Figure 2), which is thought to have a perturbed zinc binding site.[6] R175H yielded a peak H2^{175}, under conditions where wt and other tested mutants did not produce such a peak (Figure 2, Table SI−I). Removal of zinc from wt and mutants other than R175H by EDTA resulted, however, in peak H2, whereas EDTA treatment had no effect on the CPS response of the R175H mutant (Figures 4−6), providing direct evidence that the R175H mutation results in zinc loss. Peak H2 is probably related to the accessibility of cysteine residues (known to participate in the electrocatalysis) from the structurally disturbed zinc-binding region. Moreover, we were able to monitor temperature-induced conformational transitions in mutant proteins, in excellent agreement with the differential thermodynamic stabilities of these mutants.

Until recently, it was believed that proteins are denatured when adsorbed at bare metal electrodes.[41] We have shown that a protein molecule adsorbed at a bare Hg electrode charged to positive potentials (or to the potential of zero charge) does not denature at the electrode surface.[16,17,19] Denaturation may occur, however, when the potential is shifted to negative values at which the electrocatalytic reaction is taking place. In CPS the time scale is in the order of milliseconds, with the exact time depending on the current density (or I_{str} at constant electrode size) used in the experiment. Because of the high speed of the potential changes in CPS, protein denaturation does not take place at bare Hg electrodes under suitable ionic conditions.[16,17] For example, an increase in the ionic strength affects the depth of the diffuse electrode double layer, and consequent effects of the electric field result in full or partial denaturation of the protein molecules anchored at the electrode.[16] Such surface denaturation can be decreased or eliminated by adsorbing the protein at thiol SAM formed at the Hg electrode surface.[19] We have shown that using DTT SAM for modification of the Hg electrode is convenient for the analysis of p53 (Figures 2−6) and other reduced proteins[19] stored with DTT. On the other hand, other thiols can be used for the same purpose; our preliminary results suggest that using alkanethiols of different lengths and with specific end groups may increase the specificity of the analysis of proteins. Recently, we have demonstrated that the DTT-HMDE can be substituted by DTT-modified solid amalgam electrodes[19] and have developed solid amalgam electrode arrays using vacuum metal sputtering on glass surface, photolitography, and mercury amalgam formation for their fabrication.[24]

The theory of the catalytic hydrogen evolution in low MW organic compounds and proteins was developed in the middle of the 20th century,[23] that is, at a time when detailed structural information on the analyzed proteins and protein engineering techniques to obtain highly purified wild-type and mutant proteins were not available. Our data on p53 mutants show that CPS analysis can be used to study conformational transitions in proteins to complement conventional structural techniques. The method can be applied to virtually any protein and gives instant results. It is particularly useful when only limited protein amounts are available, as only picomole amounts are needed for the measurements. Further experimental and theoretical work on this topic should open the door for the wide application of electrochemistry in protein research, including proteomics and biomedicine.

ASSOCIATED CONTENT

Supporting Information. The contents of Supporting Information includes the following: (1) chronopotentiograms of native and denatured BSA at different temperatures, (2) voltammograms of wt and R175H, (3) dependence of peak H height on the concentration of wt and R175H at 23.4 °C, (4) Table I: Parameters of peak H of p53 proteins at different temperatures. This material is available free of charge via the Internet at http://pubs.acs.org.

AUTHOR INFORMATION

Corresponding Author
palecek@ibp.cz

ACKNOWLEDGMENT

We thank Caroline Blair for protein purification. This work was supported by the Medical Research Council, European Community FP6 funding, and by AS CR KAN400310651, KJB100040901, GACR P301/11/2055, Research Centre LC06036 and IBP Research Plans Nos. AV0Z50040507 and AV0Z50040702.

REFERENCES

(1) Vogelstein, B.; Lane, D.; Levine, A. J. *Nature* **2000**, *408*, 307–310.
(2) Vousden, K. H.; Prives, C. *Cell* **2009**, *137*, 413–431.
(3) Petitjean, A.; Mathe, E.; Kato, S.; Ishioka, C.; Tavtigian, S. V.; Hainaut, P.; Olivier, M. *Hum. Mutat.* **2007**, *28*, 622–629.
(4) Joerger, A. C.; Fersht, A. R. *Annu. Rev. Biochem.* **2008**, *77*, 557–582.
(5) Joerger, A. C.; Fersht, A. R. *Cold Spring Harbor Perspect. Biol.* **2010**, *2*, a000919.
(6) Joerger, A. C.; Fersht, A. R. *Oncogene* **2007**, *26*, 2226–2242.
(7) Murgida, D. H.; Hildebrandt, P. *Acc. Chem. Res.* **2004**, *37*, 854–861.
(8) Hammerich, O.; Ulstrup, J. *Bioinorganic Electrochemistry*; Springer: Dordrecht, The Netherlands, 2008.
(9) Todorovic, S.; Jung, C.; Hildebrandt, P.; Murgida, D. H. *J. Biol. Inorg. Chem.* **2006**, *11*, 119–127.
(10) Wackerbarth, H.; Zhang, J.; Grubb, M.; Glargaard, H.; Ooi, B. L.; Christensen, H. E. M.; Ulstrup, J. In *Electrochemistry of Nucleic Acids and Proteins. Towards Electrochemical Sensors for Genomics and Proteomics*; Palecek, E., Scheller, F., Wang, J., Eds.; Elsevier: Amsterdam, 2005; pp 485−516.

(11) Dorcak, V.; Palecek, E. *Anal. Chem.* **2009**, *81*, 1543–1548.
(12) Ostatna, V.; Dogan, B.; Uslu, B.; Ozkan, S.; Palecek, E. *J. Electroanal. Chem.* **2006**, *593*, 172–178.
(13) Ostatna, V.; Kuralay, F.; Trnkova, L.; Palecek, E. *Electroanalysis* **2008**, *20*, 1406–1413.
(14) Ostatna, V.; Palecek, E. *Electrochim. Acta* **2008**, *53*, 4014–4021.
(15) Palecek, E.; Ostatna, V. *Electroanalysis* **2007**, *19*, 2383–2403.
(16) Palecek, E.; Ostatna, V. *Chem. Commun.* **2009**, 1685–1687.
(17) Palecek, E.; Ostatna, V. *Analyst* **2009**, *134*, 2076–2080.
(18) Palecek, E.; Ostatna, V.; Masarik, M.; Bertoncini, C. W.; Jovin, T. M. *Analyst* **2008**, *133*, 76–84.
(19) Ostatna, V.; Cernocka, H.; Palecek, E. *J. Am. Chem. Soc.* **2010**, *132*, 9408–9413.
(20) Fojta, M.; Kubicárová, T.; Vojtesek, B.; Palecek, E. *J. Biol. Chem.* **1999**, *274*, 25749–25755.
(21) Banica, F. G.; Ion, A. In *Encyclopedia of Analytical Chemistry*; Meyers, R. A., Ed.; John Wiley and Sons: Chichester, 2000; pp 11115−11144.
(22) Heyrovsky, M. *Electroanalysis* **2004**, *16*, 1067–1073.
(23) Mairanovskii, S. G. *Russ. Chem. Rev.* **1964**, *33*, 38–55.
(24) Juskova, P.; Ostatna, V.; Palecek, E.; Foret, F. *Anal. Chem.* **2010**, *82*, 2690–2695.
(25) Brazdova, M.; Kizek, R.; Havran, L.; Palecek, E. *Bioelectrochem.* **2002**, *55*, 115–118.
(26) Joerger, A. C.; Allen, M. D.; Fersht, A. R. *J. Biol. Chem.* **2004**, *279*, 1291–1296.
(27) Nikolova, P. V.; Henckel, J.; Lane, D. P.; Fersht, A. R. *Proc. Natl. Acad. Sci. U.S.A.* **1998**, *95*, 14675–14680.
(28) Joerger, A. C.; Ang, H. C.; Fersht, A. R. *Proc. Natl. Acad. Sci. U.S.A.* **2006**, *103*, 15056–15061.
(29) Joerger, A. C.; Ang, H. C.; Veprintsev, D. B.; Blair, C. M.; Fersht, A. R. *J. Biol. Chem.* **2005**, *280*, 16030–16037.
(30) Ang, H. C.; Joerger, A. C.; Mayer, S.; Fersht, A. R. *J. Biol. Chem.* **2006**, *281*, 21934–21941.
(31) Palecek, E. *Bioelectrochem. Bioenerg.* **1992**, *28*, 71−83.
(32) Palecek, E.; Postbieglová, I. *J. Electroanal. Chem.* **1986**, *214*, 359–371.
(33) Fojta, M.; Vetterl, V.; Tomschik, M.; Jelen, F.; Nielsen, P.; Wang, J.; Palecek, E. *Biophys. J.* **1997**, *72*, 2285–2293.
(34) Palecek, E.; Jelen, F. In *Electrochemistry of Nucleic Acids and Proteins. Towards Electrochemical Sensors for Genomics and Proteomics*; Palecek, E., Scheller, F., Wang, J., Eds.; Elsevier: Amsterdam, 2005; pp 74−174.
(35) Palecek, E. *Electroanalysis* **2009**, *21*, 239–251.
(36) Doneux, T.; Dorcak, V.; Palecek, E. *Langmuir* **2010**, *26*, 1347–1353.
(37) Butler, J. S.; Loh, S. N. *Biochemistry (Moscow)* **2003**, *42*, 2396–2403.
(38) Bullock, A. N.; Henckel, J.; Fersht, A. R. *Oncogene* **2000**, *19*, 1245–1256.
(39) Zivanovic, M.; Aleksic, M.; Ostatna, V.; Doneux, T.; Palecek, E. *Electroanalysis* **2010**, *22*, 2064–2071.
(40) Loh, S. N. *Metallomics* **2010**, *2*, 442–449.
(41) Armstrong, F. A. In *Bioelectrochemistry*; Wilson, G. S., Ed.; Wiley-VCH: Weinheim, 2002; Vol. 9, pp 11−29.